Plasmonics (2018) 13:15–19
DOI 10.1007/s11468-016-0478-9

# A High-Performance Refractive Index Sensor Based on Fano Resonance in Si Split-Ring Metasurface

**Gui-Dong Liu[1] · Xiang Zhai[1] · Ling-Ling Wang[1] · Qi Lin[1] · Sheng-Xuan Xia[1] · Xin Luo[1] · Chu-Jun Zhao[1]**

Received: 19 May 2016 / Accepted: 19 December 2016 / Published online: 20 January 2017


**Abstract** We present a high-performance refractive index sensor based on Fano resonance with a figure of merit (FOM) about 56.5 in all-dielectric metasurface which consists of a periodically arranged silicon rings with two equal splits dividing them into pairs of arcs of different lengths. A Fano resonance with quality factor ~133 and spectral contrast ratio ~100% arises from destructive interference of two antiphase electric dipoles in the two arcs of the split-ring. We can turn on and/or off the Fano resonance with a modulation depth nearly 100% at the operating wavelength of 1067 nm by rotating the polarization of incident light. We believe that our results will open up avenues for the development of applications using Fano resonance with dynamically controllability such as biochemical sensors, optical switching, and modulator.

**Keywords** Dielectric metasurface · Fano resonance · Optical sensing

## Introduction

Fano resonance is originally observed in atomic physics, where interference between a discrete narrow state and a wide continuum state produces a sharp and asymmetric spectral line shape for light propagating through an originally opaque medium [1, 2]. Since it is a general wave phenomenon, Fano resonance caused by destructive interference between bright and dark modes has also been observed in plasmonic nanostructures [2–6]. Bright modes with large net dipole moments can be efficiently excited by light, while dark modes possess zero or negligible net dipole moments preventing it from direct excitation by normally incident light. Fortunately, the dark modes can be excited by near-field coupling with the bright modes. So far, numerous nanostructures have been designed to generate Fano resonances, such as disk-ring cavities [7–9], dolmen structures [9–12], and coupled clusters of nanoparticles [13]. In these cases, in order to suppressed radiative damping of bright mode, dark modes, e.g., the bonding resonance of a nanorod dimer and the multipolar resonances of a nanoring, have nearly zero net dipole moment are designed.

Fano resonances have drawn extraordinary interest due to their significant properties and are promising to develop applications in numerous areas. For example, using the strong near-field enhancement at the spectral region of dark modes or Fano minima, the plasmonic nanostructures are useful for surface-enhanced Raman scattering (SERS) [9, 13]; Since Fano resonances arise from the interference between the bright and dark modes, the plasmonic nanostructure can be used for Fano line shaping [14] by control the spectral relative region between bright and dark modes. Recently, it has been numerically and experimentally investigated that plasmonic Fano switches can be controlled by the polarization of the incident light. Chang et al. [15] report that clusters with a hemicircular central disk surrounded by a circular ring of closely spaced, coupled nanodisks yield Fano-like and non-Fano-like spectra for orthogonal incident polarization orientations since this octamer nanostructure is asymmetric and it supports a dark mode only for one polarization orientation and not for the orthogonal polarization. Zhang et al. [16] and He et al. [17] demonstrate the plasmonic Fano switches based on nanoring dimer arrays and disk-rod hybrid metasurfaces, respectively, by taking advantage of the polarization-

✉ Ling-Ling Wang
llwang@hnu.edu.cn

[1] Key Laboratory for Micro-Nano Optoelectronic Devices of Ministry of Education, School of Physics and Electronics, Hunan University, Changsha 410082, China

dependent of the coupling strength between the bright and dark modes. However, some issues have not yet been adequately addressed in the above proposed structures. First, the spectral contrast ratio is relatively low as there is a large energy gap between superradiate (bright) and subradiate (dark) modes. The spectral contrast ratio can be heightened by reducing the relative distance between bright and dark modes while the quality factor of the Fano resonance will be subsequently decreased. Second, the proposed plasmonic nanostructures based on the metals with abundant free electrons and exhibit high Joule losses leading to low-quality factor scattering or transmission responses, which will greatly reduce the performance of the switch. Fortunately, since the nonradiative losses can be effectively suppressed by substituting metallic materials by dielectric ones [18–21], the shortcomings mentioned above can be possibly overcome. Fano resonances based plasmonic nanostructures also have been widely researched in bio-chemical sensing [7–9, 22–24] on reason that the plasmonic Fano resonances are sensitive to a nearby or surrounding dielectric medium since they arise from inter-particle coupling. More importantly, thanks to much smaller line width of the Fano resonance, the performance of bio-chemical sensor based on all-dielectric metasurface can be greater optimized than plasmonic ones.

We present a high-quality factor and modulation depth Fano sensor with a figure of merit (FOM) about 56.5 based on all-dielectric metasurface which is composed of a periodically arranged silicon rings with two equal splits dividing them into pairs of arcs of different length. A Fano resonance with quality factor ~133 and spectral contrast ratio ~100% observed in the transmission spectrum arises from the destructive interference of two antiphase electric dipoles in the two arcs of the Si split-ring in a unit cell of the proposed metasurface. Furthermore, an on-to-off transmission amplitude modulation of the Fano resonance with modulation depth ~100% at the resonance wavelength of 1067 nm is achieved by rotating the polarization of the incident light. The effects of the geometric parameters on the Fano resonance are also investigated and results show that the Fano resonance can be tuned to different wavebands by changing the geometric parameters of the metasurface. Therefore, dynamic controlling of Fano resonance in this work may open up avenues for the development of applications such as bio-chemical sensing, optical switching and optical modulator.

## Theory and Simulations

Figure 1 shows the schematics of the proposed all-dielectric metasurface which is composed of a periodically arranged silicon rings with two equal splits dividing them into pairs of arcs of different length corresponding to $\beta_1 = 120°$ and

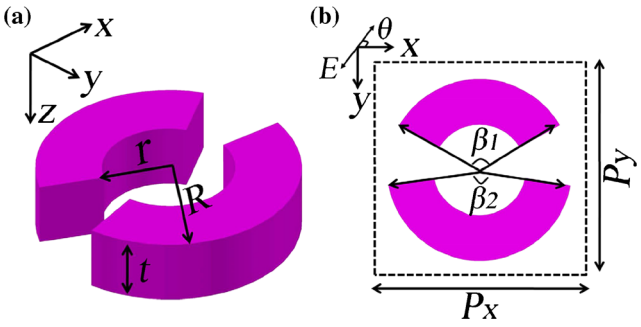


**Fig. 1** **a** Three- and **b** two-dimensional schematics of the all-dielectric metasurface which is composed of a periodically arranged silicon rings with two equal splits dividing them into pairs of arcs of different lengths. The geometrical parameters are $r$ = 150 nm, $R$ = 300 nm, $t$ = 110 nm, $\beta_1 = 120°$, $\beta_2 = 160°$, and $P = P_x = P_y = 700$ nm

$\beta_2 = 160°$. The Si split-ring has thick $t$ = 110 nm, inner radius $r$ = 150 nm, outer radius $R$ = 300 nm, and the period is $P = P_x = P_y = 700$ nm, respectively. Our results are obtained by using finite-difference time-domain (FDTD) method, where the periodic structures are illuminated by a normally incident plane wave and the angle of the polarization direction of its electric field with respect to the $x$-axis is defined as $\theta$ (see Fig. 1b). Perfectly matched layers (PML) are applied along the $z$ direction and periodic boundary conditions in the $x$ and $y$ directions. The dielectric constant of Si can be referred from Ref. [25].

Figure 2a shows the transmission spectra of the all-dielectric metasurface at normal incidence with $x$-polarization ($\theta = 0°$) obtained by FDTD method. A sharp Fano

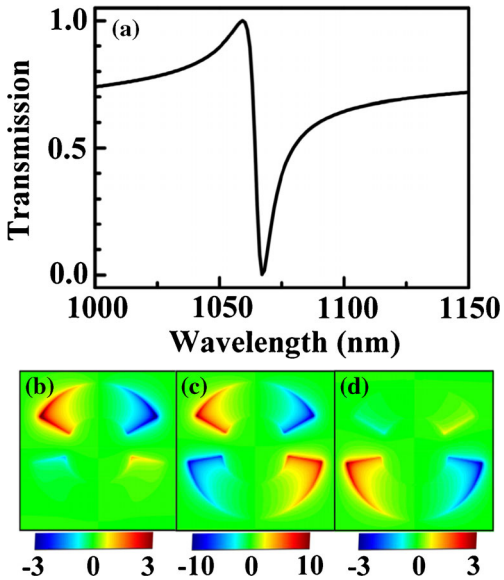


**Fig. 2** **a** The transmission spectra of the all-dielectric metasurface at normal incidence with $x$-polarization ($\theta = 0°$) obtained by FDTD method. **b** Magnitude of the $z$-component of electric field ($Ez$) distributions of the metasurface at the wavelength of **b** 1036, **c** 1067, and **d** 1097 nm. The field distributions are calculated in the $x$-$y$ plane that is 5 nm above the top surface of the metasurface

resonance appears in the transmission spectrum around 1067 nm, and the Fano profile evolves from a dip with transmission amplitude ~0 to a peak with transmission amplitude ~1 within 8 nm. In order to interpret the Fano resonance clearly, we plot the *z*-component of electric field (*Ez*) distributions in a unit cell of the proposed metasurface at wavelength of 1036, 1067, and 1097 nm, as shown in Fig. 2b, c, d, respectively. From the *Ez* field distributions at 1036 nm which is slightly below the Fano resonance wavelength, it is obvious that the minor arc of the split ring dominates its major arc oscillating in antiphase while the major arc of the split ring dominates its minor arc oscillating in antiphase at 1097 nm which is above the Fano resonance wavelength, as shown in Fig. 2b, d, respectively. The overlap of the two modes results in two almost identical but antiphase electric dipoles in the two arcs of the Si split-ring in a unit cell of the proposed metasurface leading to Fano resonance, as shown in Fig. 2c. The quality factor and spectral contrast ratio of the Fano resonance is introduced to evaluate the potential of the metasurface in optical applications. The quality factor Q, defined as the ratio of the resonance wavelength $\lambda_0$ and the full width $\Delta\lambda$ between the peak and the antipeak of the transmission ($Q = \lambda_0/\Delta\lambda$), reaches about 133 and the spectral contrast ratio [19], defined as $[(T_{peak} - T_{antipeak})/(T_{peak} + T_{antipeak})] \times 100\%$, reaches about 100%. The possessions of high-quality factor and spectral contrast ratio of the Fano resonance make the proposed metasurface a promising candidate in a series of applications where sharp resonance is essential for the performance, such as biochemical sensors [7–9, 22–24], optical filters [20], and switch [15–17].

We take advantage of the high quality factor and spectral contrast ratio of the Fano resonance, as well as the asymmetry of the proposed metasurface to design a high-performance optical switch. The transmission amplitude of the Fano resonance can be modulated by rotating the polarization orientations of the incident light. The transmission spectra of the proposed metasurface obtained for different polarization orientations of the incident light are presented in Fig. 3a. As the $\theta$ is increased from 0° to 90°, the transmission undergoes strong modulations, with transmission dips gradually shrinks without a notable wavelength shift. Finally, the Fano resonance disappeared completely and the transmission amplitude of 90% at the wavelength of 1067 nm is achieved when the polarization of the incident light is along the *y*-axis ($\theta = 90°$). The resultant modulation depth [16], defined as $|(T_{on} - T_{off})/T_{on}| \times 100\%$, reaches nearly 100%, where $T_{on}$ and $T_{off}$ represent the maximized transmission amplitude ~0.9 at 1067 nm as $\theta = 90°$ and the minimized transmission amplitude ~0 at 1067 nm as $\theta = 0°$, respectively. Thanks to the ultrahigh modulation depth, the high-quality factor, and spectral contrast ratio of the Fano resonance, this optical switch in the proposed all-dielectric metasurface will have a better performance than the plasmonic Fano switches reported in Refs. 15–17.

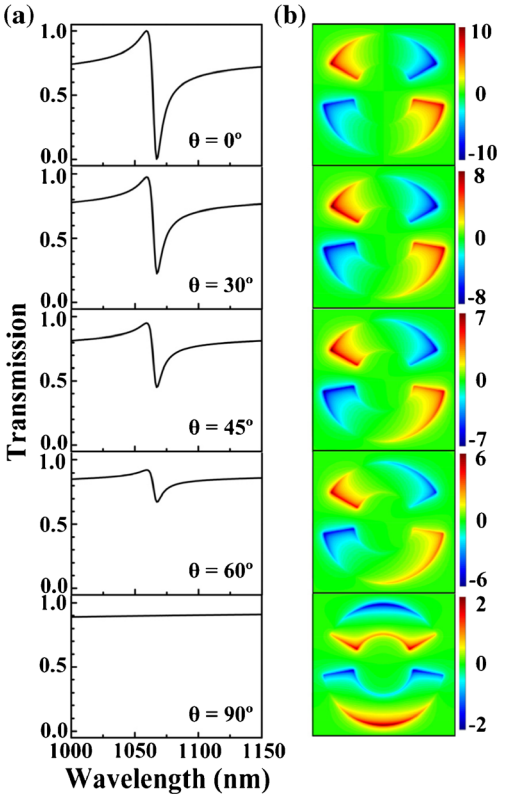


**Fig. 3** **a** The transmission spectra of the proposed metasurface at different polarization $\theta$ obtained by FDTD method. **b** Corresponding simulated in-plane electric field (*Ez*) distribution monitored at the dip of transmission ($\lambda_0 = 1067$ nm). The field distribution is calculated in the *x*-*y* plane that is 5 nm above the top surface of the all-dielectric metasurface

To explore the underlying physics of this polarization-dependent behavior, we calculated the *z*-component distribution of the electric near-field in the *x*-*y* plane that is 5 nm above the top surface of the proposed all-dielectric metasurface at the wavelength of 1067 nm for different polarization angles, as shown in Fig. 3b. When the electric field is polarized along *x*-axis, i.e. $\theta = 0°$, at the Fano resonance ($\lambda_0 = 1067$ nm), *x*-components of the two electric dipole moments in two parts of the split-ring are antiphase and have almost the same amplitude while *y*-components are zero. With the increase of $\theta$, *y*-components of the two electric dipole moments are inphase and increased in amplitude while antiphase *x*-components of the two electric dipole moments are gradually decreased in amplitude, and thus Fano resonances are gradually faded off. As the electric field of the incident light polarized along *y*-axis, i.e. $\theta = 90°$, at the wavelength of 1067 nm, the net dipole moment in the split-ring has zero *x*-components while its *y*-components are inphase leading to the disappearance of Fano resonance.

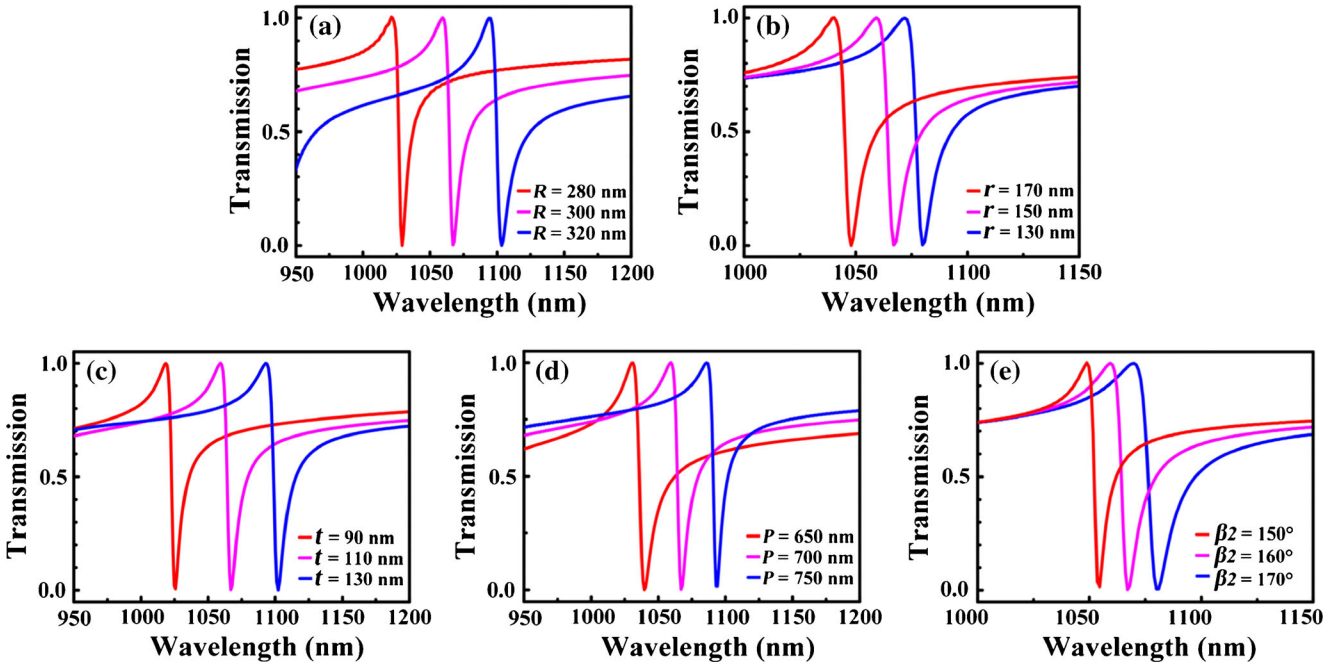


**Fig. 4** The transmission spectra of the proposed metasurface for varied outer radius $R$ (**a**), and inner radius $r$ (**b**), and thick $t$ (**c**), and period $P$ (**d**), and $\beta_2$ (**e**). The incident plane wave propagates along the $z$-axis, and the polarization is along the $x$-axis ($\theta = 0°$)

We also investigated the effects of the geometric parameters of the proposed metasurface on the Fano resonance. Figure 4a–e shows the transmission spectra of the proposed metasurface with various $R$, $r$, $t$, $P$, $\beta_2$, respectively, and the other geometric parameters are fixed as Fig. 1. The incident plane wave propagates along the $z$-axis and the electric field is polarized along the $x$-axis. As shown in Fig. 4a, b, respectively, decreases of the outer radius $R$ or increases of the inner radius $r$ lead to a blueshift of the Fano resonance due to the decrease of effective line width of the two arcs of the split-ring. Figure 4c illustrates that the Fano resonance redshifts as the Si split-ring gets thicker on reason that a larger fraction of field is inside the proposed metasurface. Increase of period $P$ also will lead to the redshift of the Fano resonance as shown in Fig. 4d. When $\beta_2$ increases from 150° to 170° (see Fig. 4e), the Fano resonance redshifts because of the increase of effective length and the slight reduction of quality factor is due to the increase the asymmetry between the minor and major arcs of the Si split-ring. It is worth noting that the resonance wavelength of Fano resonance could be changed by adjusting the geometric parameters of the metasurface while the spectral contrast ratio still remains nearly 100%. Thus, the operating wavelength of optical device based on the Fano resonance can be designed by optimizing and amplifying or reducing the geometric parameters of the metasurface.

In fact, the calculations above are based on self-standing all-dielectric metasurface, while the surrounding medium in applications may not be air. Herein, we investigated the influence of surrounding medium with different refractive index $n$ on the Fano resonance. Figure 5a represents the simulated transmission spectra of the proposed metasurface with different refractive index of the surrounding media, while the other geometric parameters of the metasurface are the same as Fig. 1. Increases of refractive index $n$ lead to a redshift of the Fano resonance while it has little influence on the quality factor and spectral contrast ratio of the Fano resonance as shown in Fig. 5a. A spectral shift relative to air ($n = 1.0$) verse the RI of the surrounding media is potted in Fig. 5b, and a

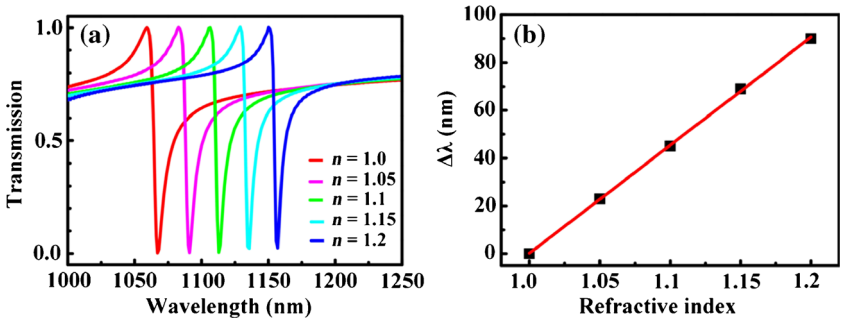


**Fig. 5** **a** The transmission spectra for the proposed metasurface with different surrounding media. **b** The resonance wavelength shift of the Fano resonance relative to air ($n = 1.0$)

linear fit to the data gives that the wavelength shift per refractive index units of the Fano resonance $S$ is 452 nm/RIU. The figure of merit (FOM) is used for evaluating the performance of a refractive index sensor [3]:

$$\mathrm{FOM} = \frac{S\left(\mathrm{nm}/\mathrm{RIU}\right)}{\Delta\lambda(\mathrm{nm})}$$

where $\Delta\lambda$ is the full width between the peak and the antipeak of the transmission. The $\Delta\lambda$ of the Fano resonance is about 8 nm and the FOM is about 56.5. The FOM is much larger than sensor based on plasmonic nanostructure [7–9, 22–24], it certificates that the performance of bio-chemical sensor based on all-dielectric metasurface greater than plasmonic ones.

To conclude, we presented a high-quality factor and modulation depth Fano sensor with a figure of merit (FOM) about 56.5 based on all-dielectric metasurface which is composed of a periodically arranged silicon rings with two equal splits dividing them into pairs of arcs of different length. The Fano resonance with quality factor ~133 and spectral contrast ratio ~100% observed in the transmission spectrum arose from the destructive interference of two antiphase electric dipoles in the two arcs of the Si split-ring in a unit cell of the proposed metasurface. Furthermore, an on-to-off transmission amplitude modulation of the Fano resonance with modulation depth ~100% at the resonance wavelength of 1067 nm was achieved by rotating the polarization of the incident light. The effects of the geometric parameters on the Fano resonance were also investigated, and results show that the Fano resonance can be tuned to different wavebands by changing the geometric parameters of the metasurface. Therefore, dynamic controlling of Fano resonance in this work may open up avenues for the development of applications such as bio-chemical sensing, optical switching, and optical modulator.

**Acknowledgements** This work was supported by the National Natural Science Foundation of China (Grant Nos. 61505052, 61176116, 11074069).

## References

1. Ugo F (1961) Effects of configuration interaction on intensities and phase shifts. Phys Rev 124:1866–1878
2. Miroshnichenko AE, Flach S, Kivshar YS (2010) Fano resonances in nanoscale structures. Rev Mod Phys 82:2257–2298
3. Liu GD, Zhai X, Wang LL, Wang BX, Lin Q, Shang XJ (2016) Actively tunable Fano resonance based on a T-shaped graphene Nanodimer. Plasmonics 11:381–387
4. Lin Q, Zhai X, Wang LL, Wang BX, Liu GD, Xia SX (2015) Combined theoretical analysis for plasmon-induced transparency in integrated graphene waveguides with direct and indirect couplings. Europhys Lett 111:34004
5. Hu C, Wang LL, Lin Q, Zhai X, Ma XY, Han T, Du J (2016) Tunable double transparency windows induced by single subradiant element in coupled graphene plasmonic nanostructure. Appl Phys Express 9:052001
6. Xia SX, Zhai X, Wang LL, Sun B, Liu JQ, Wen SC (2016) Dynamically tunable plasmonically induced transparency in sinusoidally curved and planar graphene layers. Opt Express 24:17886–17899
7. Liu SD, Yang Z, Liu RP, Li XY (2011) High sensitivity localized surface plasmon resonance sensing using a double split nanoring cavity. J Phys Chem C 115:24469–24477
8. Fu YH, Zhang JB, Yu YF, Luk'yanchuk B (2012) Generating and manipulating higher order Fano resonances in dual-disk ring plasmonic nanostructures. ACS Nano 6:5130–5137
9. Zhang Q, Wen XL, Li GY, Ruan QF, Wang JF, Xiong QH (2013) Multiple magnetic mode-based Fano resonance in split-ring resonator/disk nanocavities. ACS Nano 7:11071
10. Zhang S, Genov DA, Wang Y, Liu M, Zhang X (2008) Plasmon-induced transparency in metamaterials. Phys Rev Lett 101:047401
11. Shi X, Han DZ, Dai YY, Yu ZF, Sun Y, Chen H, Liu XH, Zi J (2013) Plasmonic analog of electromagnetically induced transparency in nanostructure graphene. Opt Express 21:28438–28443
12. Cheng H, Chen SQ, Yu P, Duan XY, Xie BY, Tian JG (2013) Dynamically tunable plasmonically induced transparency in periodically patterned graphene nanostrips. Appl Phys Lett 103:203112
13. Ye J, Wen FF, Sobhani H, Lassiter JB, Dorpe PV, Nordlander P, Halas NJ (2012) Plasmonic nanoclusters: near field properties of the Fano resonance interrogated with SERS. Nano Lett 12:1660–1667
14. Verellen N, Dorpe PV, Huang C, Lodewijks K, Vandenbosch GAE, Lagae L, Moshchakov VV (2011) Plasmon line shaping using nanocrosses for high sensitivity localized surface plasmon resonance sensing. Nano Lett 11:391–397
15. Chang WS, Lassiter JB, Swanglap P, Sobhani H, Khatua S, Nordlander P, Halas NJ, Link S (2012) A plasmonic Fano switch. Nano Lett 12:4977–4982
16. Zhang L, Dong ZG, Wang YM, Liu YJ, Zhang S, Yang JKW, Qiu CW (2015) Dynamically configurable hybridization of plasmon modes in nanoring dimer arrays. Nanoscale 7:12018–12022
17. He JN, Wang JQ, Ding P, Fan CZ, Arnaut LR, Liang EJ (2015) Optical switching based on polarization tunable plasmon-induced transparency in disk/rod hybrid metasurfaces. Plasmonics 10:1115–1121
18. Zhang JF, Lin W, Zhu ZH, Yuan XD, Qin SQ (2014) Strong field enhancement and light-matter interactions with all-dielectric metamaterials based on split bar resonators. Opt Express 25:30889–30898
19. Zhao WY, Jiang H, Liu BY, Jiang YY, Tang CC, Li JJ (2015) Fano resonance based optical modulator reaching 85% modulation depth. Appl Phys Lett 107:171109
20. Zhao WY, Leng XD, Jiang YY (2015) Fano resonance in all-dielectric binary nanodisk array realizing optical filter with efficient linewidth tuning. Opt Express 23:6858–6966
21. Muhammad N, Khan AD (2015) Tunable Fano resonances and electromagnetically induced transparency in all-dielectric holey block. Plasmonics 10:1687–1693
22. Zhan Y, Lei DY, Li X et al (2014) Plasmonic Fano resonances in nanohole quadrumers for ultra-sensitive refractive index sensing. Nanoscale 6:4705–4715
23. König M, Rahmani M, Zhang L et al (2014) Unveiling the correlation between nanometer-thick molecular monolayer sensitivity and near-field enhancement and localization in coupled plasmonic oligomers. ACS Nano 8:9188–9198
24. Yong Z, Lei DY, Lam CH et al (2014) Ultrahigh refractive index sensing performance of plasmonic quadrupole resonances in gold nanoparticles. Nanoscale Res Lett 2014(9):1–6
25. Palik ED (1998) Handbook of optical constants of solids, vol 3. Academic press, Boston, p 653